Meteoritics & Planetary Science 38, Nr 3, 445–455 (2003)
Abstract available online at http://meteoritics.org

Cloud Creek structure, central Wyoming, USA: Impact origin confirmed

Donald S. STONE[1*] and Ann M. THERRIAULT[2]

[1]6178 South Lakeview Street, Littleton, Colorado 80120, USA
[2]Geological Survey of Canada, 601 Booth Street, Room 227, Ottawa, Ontario K1A 0E8, Canada
[*]Corresponding author. E-mail: don@dsstone.com

(Received 1 August 2002; revision accepted 16 December 2003)

Abstract–The circular Cloud Creek structure in central Wyoming, USA is buried beneath ~1200 m of Mesozoic sedimentary rocks and has a current diameter of ~7 km. The morphology/morphometry of the structure, as defined by borehole, seismic, and gravity data, is similar to that of other buried terrestrial complex impact structures in sedimentary target rocks, e.g., Red Wing Creek in North Dakota, USA. The structure has a fault-bordered central peak with minimum diameter of ~1.4 km, composed predominantly of Paleozoic carbonates thickened by thrust faulting and brecciation, and is elevated some 520 m above equivalent strata beyond the outer rim of the structure. There is a ~1.6 km wide annular trough sloping away from the central peak (maximum structural relief, 300 m) and terminated by a detached, fault-bounded, rim anticline. The youngest rocks within the structure are Late Triassic (Norian?) clastics and these are overlain unconformably by post-impact Middle Jurassic (Bathonian?) sandstones and shales. Thus, the formation of the Cloud Creek structure is dated chronostratigraphicly as ~190 ± 20 Ma.

Reported here for the first time are measurements of planar deformation features (PDFs) in shocked quartz grains in thin sections made from drill cuttings recovered in a borehole drilled at the southern perimeter of the central peak. Other, less definitive microstructures consistent with impact occur in samples collected from boreholes drilled into the central peak and rim anticline. The shock-metamorphic evidence confirms an impact origin for the Cloud Creek structure.

INTRODUCTION

Located 48 km northwest of Casper, near the center of the Casper Arch in central Wyoming (43°10.6′N, 106°42.5′W; Fig. 1), the circular Cloud Creek structure occurs in sedimentary rocks and is buried beneath the Triassic/Jurassic (TR-J) unconformity at an average depth of ~1200 m below the present surface. The Casper Arch and the secondary structures distributed across it (Fig. 1) are Laramide (Paleocene/Eocene) compressional features (Skeen and Ray 1983; Thompson and Hill 1986; Blackstone 1990; Brown 1993; Stone 1969, 1993, 2002), and the Cloud Creek structure lies between two Laramide, basement-involved, fault-related folds: the Sulphur Springs and North Casper Creek anticlines (Figs. 1 and 2). Morphology of the Cloud Creek structure is quite well defined by borehole, reflection seismic and gravity data. Although there has been significant post-impact, pre-Middle Jurassic erosion, and an important Laramide compressional overprint is evident, the morphology of the Cloud Creek structure is nevertheless clearly comparable to that of a complex impact structure.

At the time of the proposed bolide impact, country rocks in the Cloud Creek area consisted of a column of Triassic and Paleozoic sedimentary formations, with an estimated original thickness of ~900 m, overlying Precambrian crystalline basement (Fig. 3). An unknown thickness of rocks was removed by erosion prior to the deposition of the Middle Jurassic Sundance Formation over the eroded Cloud Creek structure. As the proposed impact probably occurred on an exposed, lithified part of the non-marine Chugwater Formation, it is very unlikely that there was any significant amount of standing water present at the impact site.

Unambiguous shock-metamorphic evidence for a hypervelocity impact origin was not reported in an earlier published description and analysis of the Cloud Creek structure (Stone 1999). However, further study of the original thin sections, made from selected drill cutting samples from a borehole drilled on the southern perimeter of the central peak of the Cloud Creek structure, has resulted in the discovery of planar deformation features (PDFs) in scarce quartz grains. Other microstructures suggestive of an impact origin are noted in drill cuttings from the central peak and rim of the Cloud Creek structure. We present this new shock-metamorphic evidence, along with a summary of the

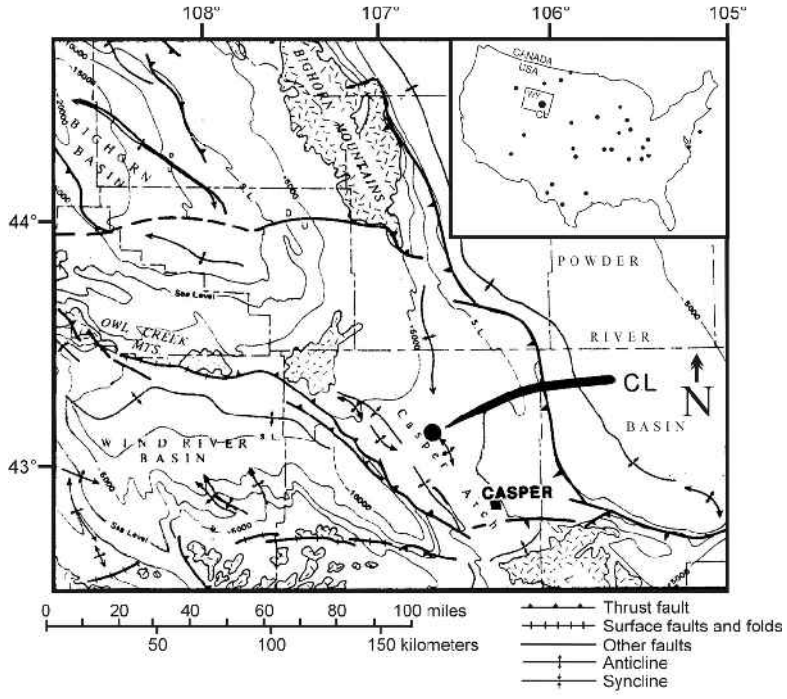

Fig. 1. Location of the Cloud Creek impact structure (CL) on a regional tectonic map of central Wyoming, United States. Contours (in ft) are on the Cretaceous Dakota Formation. The stippled areas are Precambrian crystalline rocks. The inset shows the continental US with Cloud Creek in relation to other impact structures (confirmed, probable, possible) as black dots. (Modified from Stone 1999.)

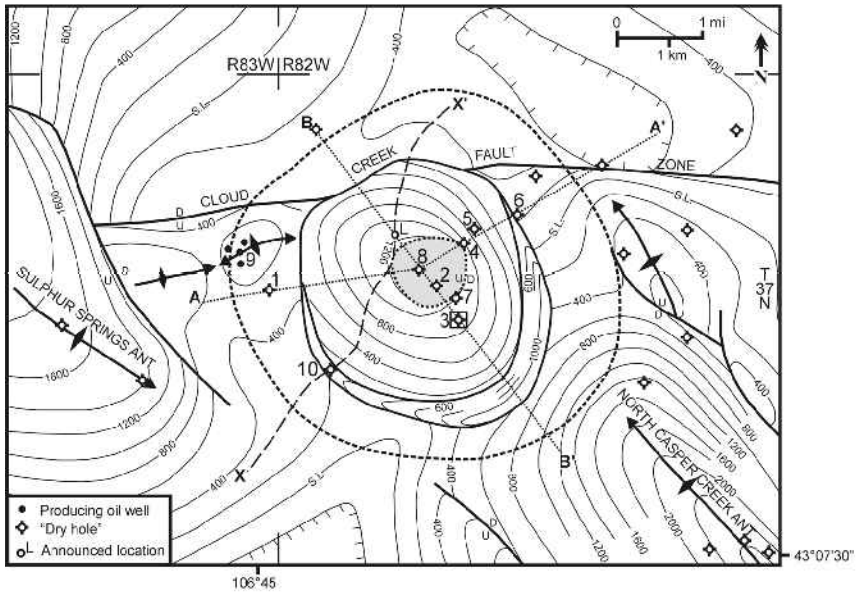

Fig. 2. Structural contour map on the Pennsylvanian Tensleep Formation (modified from Stone 1999). Contour interval is 200 ft (60 m). Base level datum is mean sea level (S.L.). The trace of the outer rim fault zone just below the TR-J unconformity is marked by the largest dashed circle. The smallest dashed circle near the center of the map is the annular fault zone that encircles the central peak. Within this annular peak-ring fault zone (the area marked by a gray stippled pattern), the contoured Tensleep horizon is missing (by ejection and/or erosion) and Amsden Formation rocks are uplifted and truncated at the TR-J unconformity. Note also the fault-bordered rim anticline along the southern perimeter of the Cloud Creek structure at the Tensleep level. Outside the crater limits, structural features are of post-impact, Laramide origin. The small area of closed 600 ft contour enclosing four producing wells outlines the recently discovered Lost Dome oil field. These wells produce oil from the Tensleep Sandstone reservoir beneath the outer rim (fault zone) of the Cloud Creek structure (cf., Fig. 5a). Structural cross-sections A-A′ and B-B′ (Fig. 5) are shown as fine dotted lines and the location of seismic profile X-X′ (Fig. 9) is indicated by the dashed north-south line. Boreholes within the Cloud Creek structure are shown with "dry hole" symbols and numbers that match the borehole list in Table 1.

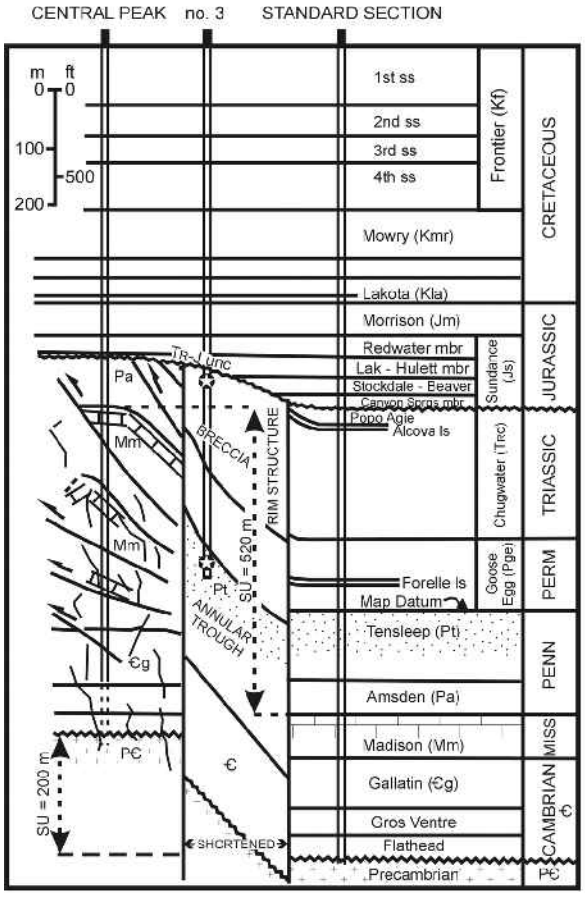

Fig. 3. Comparison of the "standard" stratigraphic column on the Casper Arch (based on the log from Pure Oil Company State #1, SE/SE Sec. 36, T37N, R82W, a Precambrian test) and the section found in the central peak (from True Oil Company #32–17, nr 8 in Table 1) of the Cloud Creek impact structure. There is no horizontal scale and the area representing the annular trough is foreshortened. Stratigraphic uplift (SU) of the Madison Formation in the central peak area above its normal elevation outside the crater is ~520 m. At the TR-J unconformity, there is progressive onlap of Sundance members over and around the central peak. The stars mark the approximate stratigraphic depth-locations of the drill cuttings from borehole nr 3 (Atlantic Refining #1 Delaney State) in which PDFs are identified. Formation symbols used on the structural cross-sections (Figs. 5 and 10) and seismic profile (Fig. 7b) are shown in parentheses along the "standard section." (Modified from Stone 1999.)

morphologic and morphometric data, and propose that the Cloud Creek structure be added to the list of confirmed terrestrial impact structures.

CRATER MORPHOLOGY/MORPHOMETRY

Borehole Stratigraphy

Stratigraphic control is provided by wireline and lithologic logs from ten deep boreholes that were drilled by oil and gas operators into or through some part of the Cloud Creek structure, and also from numerous boreholes drilled in the surrounding area (Table 1). Measured from the Upper Cretaceous Cody Shale at the surface, the normal Phanerozoic stratigraphic section above Precambrian basement and beyond the perimeter of the Cloud Creek structure includes ~1900 m of Mesozoic clastics and Paleozoic carbonates and sandstones (Fig 3). Directly below the TR-J unconformity within the Cloud Creek structure, these rocks are fractured, faulted, and/or brecciated in a manner typical of terrestrial complex impact structures (cf., Melosh 1989; Grieve 1991). Based on the implied time gap at the TR-J unconformity (Fig. 4), the proposed impact event is chronostratigraphically dated as 190 ± 20 Ma.

Above the TR-J unconformity, there is very little thickness variation in the marine Mesozoic section across the Cloud Creek structure, except in the Lower Sundance members at the base of the Jurassic. These shallow marine, lower Sundance members progressively lap out locally around the buried-hill topography of the central peak, cutting out ~75 m of basal Sundance section over the eroded crest of the central peak (Figs. 3 and 5).

Geophysical Data

Several reflection seismic profiles transect the Cloud Creek structure and provide control for the three-dimensional (3D) morphology of the Cloud Creek structure outlined here (for a map showing the location of all the seismic profiles, see Stone 1999; and Fig. 7 herein for an example profile). These two-dimensional (2D) seismic profiles are of generally fair to good quality except in the area of the central peak, where seismic resolution is poor. The structural contour map (Fig. 2) and structural cross-sections (Fig. 5) are part of a regional structural interpretation of the central Casper Arch (by the senior author) that is based on the integration of depth-migrated seismic profiles with all the relevant borehole data.

Potential fields data have also been reviewed in this study. Cloud Creek's central peak, like the central peak of the time-equivalent and morphologically similar Red Wing Creek impact structure in North Dakota (Brenan, Peterson, and Smith 1975), is expressed as a positive residual gravity anomaly (Fig. 5b). The aeromagnetic data over Cloud Creek, however, cannot be unambiguously interpreted. (See residual gravity and aeromagnetic maps in Stone 1999).

Description of Crater Elements

Most of the morphologic/structural elements that characterize terrestrial complex impact craters are recognizable at Cloud Creek. These include a rim anticline bordered by downward-converging, outer and inner circumferential ring faults, an annular trough, and an uplifted central peak encircled by one or more steeply dipping faults.

Table 1. Data compilation for wells drilled within or through parts of the Cloud Creek structure.

Nr	Well name	Location	Date	Elevation @ Kelly Bushing[a]	Total depth; Fm[b] @ Total depth	Depth of top of Sundance Fm	Depth of TR-J unconformity	Depth of top of Tensleep Fm
1	Husky Oil Co. Unit 2	NE SE sec 13 T37N, R83W	1/55	1557 m	1592 Pt	1109 m	1146 m	1567 m
2	H. Brown[c] Govt 1	NE SE sec 17 T37N, R82W	12/58	1800 m	1617 Cg	1090 m	1137 m	–
3	Atlantic Refining[c] Delaney State 1	SW SW sec 16 T37N, R82W	7/59	1748 m	1513 Pt	1103 m	1164 m	1473 m
4	Klaenhammer State 1	NW NW sec 16 T37N, R82W	8/71	1743 m	1522 Pt	1079 m	1183 m	1489 m
5	True Oil Co.[c] Anderson Draw 1	SW SW sec 9 T37N, R82W	1/72	1726 m	1623 Cg	1103 m	1173 m	1593 m
6	Oil Resources[c] Anderson Draw 2	NE SE sec 9 T37N, R82W	2/74	1697 m	1798 Pt	1055 m	1209 m	1773 m
7	Klaenhammer State 2	NW SW sec 16 T37N, R82W	8/78	1763 m	1458 Pt	1088 m	1148 m	1329 m
8	True Oil Co. Carp. Fed. 32–17	SW NE sec 17 T37N, R82W	9/89	1802 m	1677 Cg	1088 m	1135 m	–
9	Breitburn Eng.[c] Lost Dome Fed. 1	SW NE sec 13 T37N, R83W	2/98	1688 m	1522 Pt	1000 m	1091 m	1490 m
10	M. Brown Bullseye Fed. 1	NW SE sec 19 T37N, R83W	2/99	1767 m	1558 TRc	1128 m	1219 m	–

[a]Usually about 4 m above the ground elevation.
[b]Fm = formation.
[c]Drill cuttings stored at U.S. Geological Survey Core Library in Lakewood, Colorado, USA.

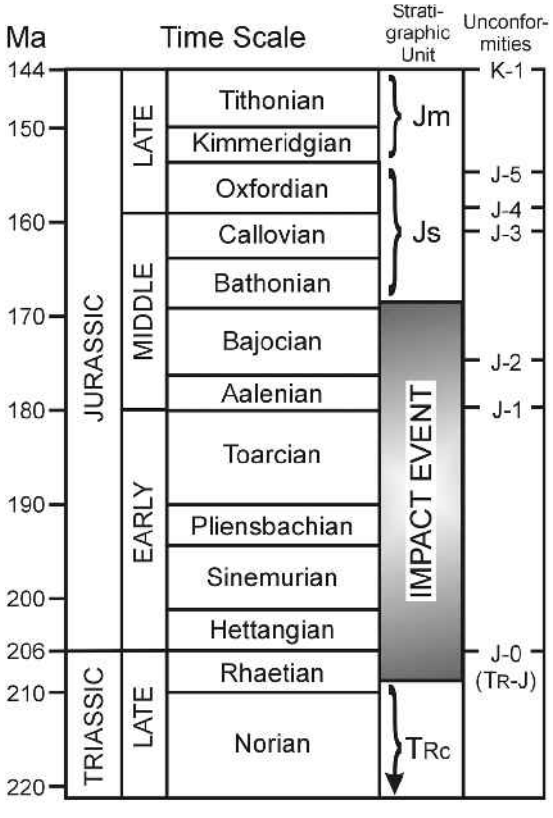

Fig. 4. Time-stratigraphic/geochronologic diagram (time scale after Geological Society of America 1998) showing stratigraphic divisions, bracketed time gap (shaded) during which the impact event occurred, formation symbols, and Jurassic unconformities after Pipiringos and O'Sullivan (1978). Jm = Morrison Formation; Js = Sundance Formation; TRc = Chugwater Formation. (Modified from Stone 1999.)

Some morphometric measurements for the Cloud Creek structure are listed in Table 2.

The Cloud Creek structure is nearly circular in plan view, but with a slight NNW-SSE elongation. It has a current rim diameter of ~7 km, measured to the outer margin of the rim anticline just below the TR-J unconformity on seismic profiles (Fig. 7).

Central Peak

There is a well-developed central peak comprised predominantly of uplifted, brecciated, fractured, and faulted Mississippian and Pennsylvanian carbonate and clastic rocks (Fig. 3). Within this central peak, data from boreholes nr 2 and 8 (Table 1; Fig. 2) indicate that the thickness of the Madison Limestone is expanded along multiple thrust faults and fractures to more than four times normal. Based on the present interpretation of the seismic data, the diameter of the central peak is ~1.4 km, measured at the Tensleep level, about half way down from the truncated crest. Stratigraphic uplift (SU) of the structurally highest Madison carbonate is ~520 m above its normal structural position outside the Cloud Creek structure. SU at the level of the deeper Cambrian/Precambrian unconformity is estimated at ~200 m (Fig. 3), based on a stratigraphic projection (~200 m) to the top of the Precambrian from the bottom of borehole Nr 8 in the central peak. A distinguishing morphologic characteristic of impact structures is that they are rootless, meaning that SU must decrease downward to zero at the base of the crater. This is especially clear where the impact structure occurs within a thick sedimentary column (e.g., at Red Wing Creek). At Cloud Creek, SU decreases downward into upper Precambrian crystalline rocks because the target sedimentary

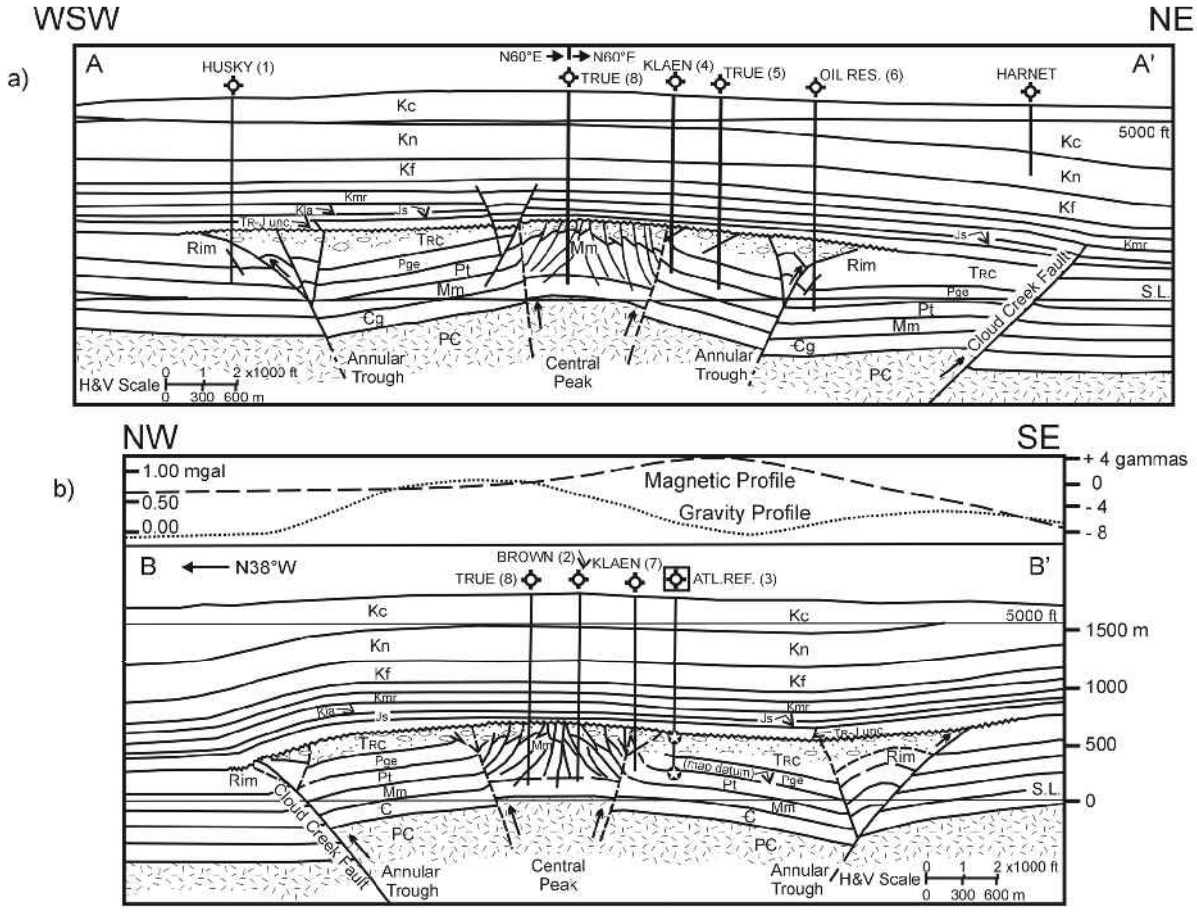

Fig. 5. True-scale structural cross-sections: a) A-A′ (WSW-NE) and b) B-B′ (NW-SE). Locations are shown in Fig. 2. The sections intersect at the True Oil Company #32–17 borehole (nr 8 in Table 1) in the central peak area of the Cloud Creek structure. The faulting and fracturing details within the central peak are idealized. Note the gravity and magnetic profiles at the top of section B-B′. Off the southeast edge of the central peak, the dry hole symbol for the Atlantic Refining Delaney State #1 borehole (nr 3 in Table 1) where PDFs were found (marked by stars) is enclosed by a small rectangle and the stratigraphic depth-location of the PDF sample by black dots. Numbers match the borehole list in Table 1 in which details are given. Formation symbols are identified in Fig. 3. Also, Kn = Niobara Shale and Kc = Cody Shale. (Modified from Stone 1999.)

column was thinner than the depth of penetration of the shock wave and the base of the developed crater. However, general seismic transparency of Precambrian crystalline basement on the Casper Arch precludes the possibility of identifying the base of the Cloud Creek crater within the affected Precambrian basement. (See comparison of seismic profiles across Cloud Creek, Red Wing Creek, and Chimney Prospect impact structures, Fig. 9, in Stone 1999).

Post-impact, Middle Jurassic Sundance sandstones and shales onlap and cover the eroded, subcropping, Pennsylvanian Amsden rocks over the crest of the central peak. This stratigraphic geometry indicates that at least 600 m of Triassic, Permian, and Pennsylvanian strata were removed by ejection at impact followed by erosion, and that the "buried-hill" topography of the central peak was formed before the deposition of Middle Jurassic sediments (Figs. 3 and 4).

The current interpretation of seismic and borehole data suggests that the central peak is encircled by a steeply dipping fault zone, which, although shown dipping inward (Figs. 5, 6, and 7), could alternatively be interpreted as dipping outward, as the quality of the seismic data in the area of the central peak is poor (cf., Pilkington and Grieve 1992).

Annular Trough

Seismic and borehole data show that an annular trough, 1200 to 1600 m wide, dips away from the central peak at about 10° on the Tensleep horizon (Fig. 2) and terminates beneath the rim anticline or outer perimeter fault zone. On the Tensleep horizon, the maximum structural elevation drop across the annular trough is ~300 m. Seismic data do not image any important faulting below the stratigraphic level of the Permian Goose Egg Formation within the trough area (although some small faults probably exist here).Within the upper Chugwater red shale/siltstone section, there are "disturbed sections" that

Table 2. Morphometric measurements of the Cloud Creek impact structure.

Morphometric element	Dimension
Diameter @ TR-J unconformity	~7 km
Circumference @ TR-J unconformity	22 km
Area @ TR-J unconformity	39 km^2
Burial depth	1090 to 1200 m
Central peak	
Diameter	1.4 km[a]
Circumference	4.4 km[a]
Stratigraphic uplift (SU) @ Madison Fm	~520 m[b]
Stratigraphic uplift (SU) @ Precambrian	~200 m[b]
Annular trough	
Average width	1.6 km[a]
Maximum relief	300 m[a]
Circumference	15 km[a]
Rim anticline	
Maximum width	610 m[a]
Maximum relief (inside bounding concentric faults)	180 m[b]

[a]Measured from Fig. 2.
[b]Measured from Fig. 3.

are characterized by chaotic dips (generally increasing near the central peak) on seismic profiles and in dipmeter surveys and by an absence of recognizable log correlations. This suggests that much of the shallower, intracrater section is composed of breccia fill (Fig. 5).

Rim Anticline

A rim anticline encircles the Cloud Creek crater at the level of the Upper Triassic Chugwater beds just below the TR-J unconformity. Several oil industry boreholes have penetrated the Cloud Creek rim anticline to provide control for the seismic interpretation (Fig. 2). Both limbs of this rim anticline are bordered by inward-dipping fault zones that converge downward. At the deeper Tensleep level, the rim anticline narrows considerably (Fig. 5) and, along the northern rim of the crater, apparently detaches above the Tensleep horizon (Fig. 2). Also, it appears that pre-Laramide erosion was deeper over the northern half of the Cloud Creek structure than over the southern half (Fig. 5b).

Seismic interpretation indicates that the rim anticline is detached above the Madison horizon around the entire crater circumference. Below this detachment, the shallower rim anticlinal structure gives way to a down-to-the-crater extentional fault zone along much of the southern perimeter of the crater. Along the northern crater perimeter, however, there has been Laramide inversion of the east-west trending part of the outer rim fault and this fault segment merges with, and becomes part of, the regional east-west trending Cloud Creek fault zone (which is thought to have a Precambrian ancestry). As a result of Laramide fault inversion, the Cloud Creek impact structure is now upthrown to the south along this composite fault zone (Fig. 5b). When the structure is restored to pre-Jurassic time by removing Laramide folding of the post-impact Mesozoic strata over the Cloud Creek structure, Laramide displacement on the composite Cloud Creek Fault zone is reversed and becomes downthrown to the crater at the basement level (Fig. 6).

Morphometric Relationships

Numerical relationships between morphometric measurements taken from the structural interpretation of the Cloud Creek structure presented here are consistent with those reported from other confirmed complex impact structures. For example, the apparent 520 m of stratigraphic uplift (SU) of the central peak, measured at the top of the Madison Formation (now less than prior to erosion) is near the 8% of the current 7 km diameter of the crater indicated as typical for complex impact craters by Melosh (1989). However, an unknown but significant amount of erosion of the original Cloud Creek impact structure occurred before deposition of the Jurassic Sundance Formation as indicated by the apparent absence of an elevated rim and ejecta blanket

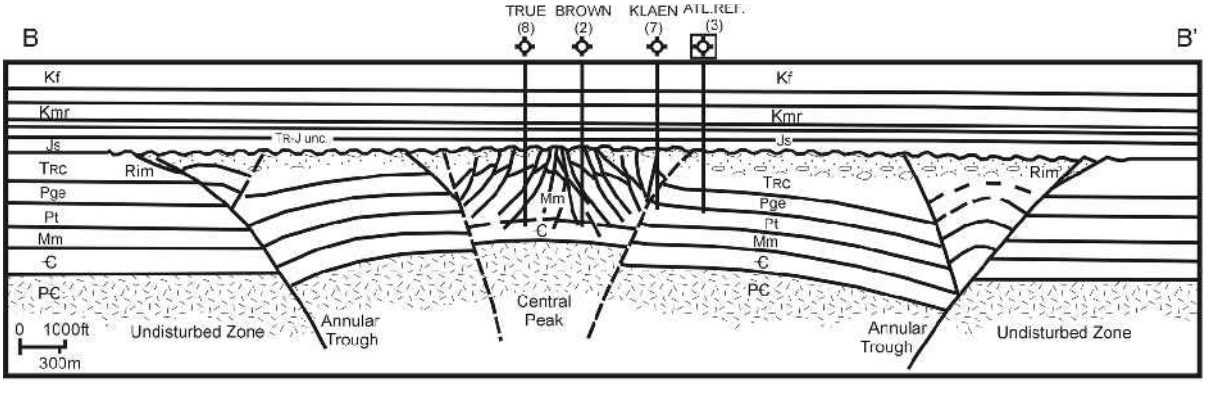

Fig. 6. Structural cross-section B-B′ (Fig. 5b) restored by flattening on the Sundance datum to remove the effects of Laramide deformation. Numbers match borehole list in Table 1 in which details are given. Formation symbols are identified in Fig. 3. (Modified from Stone 1999.)

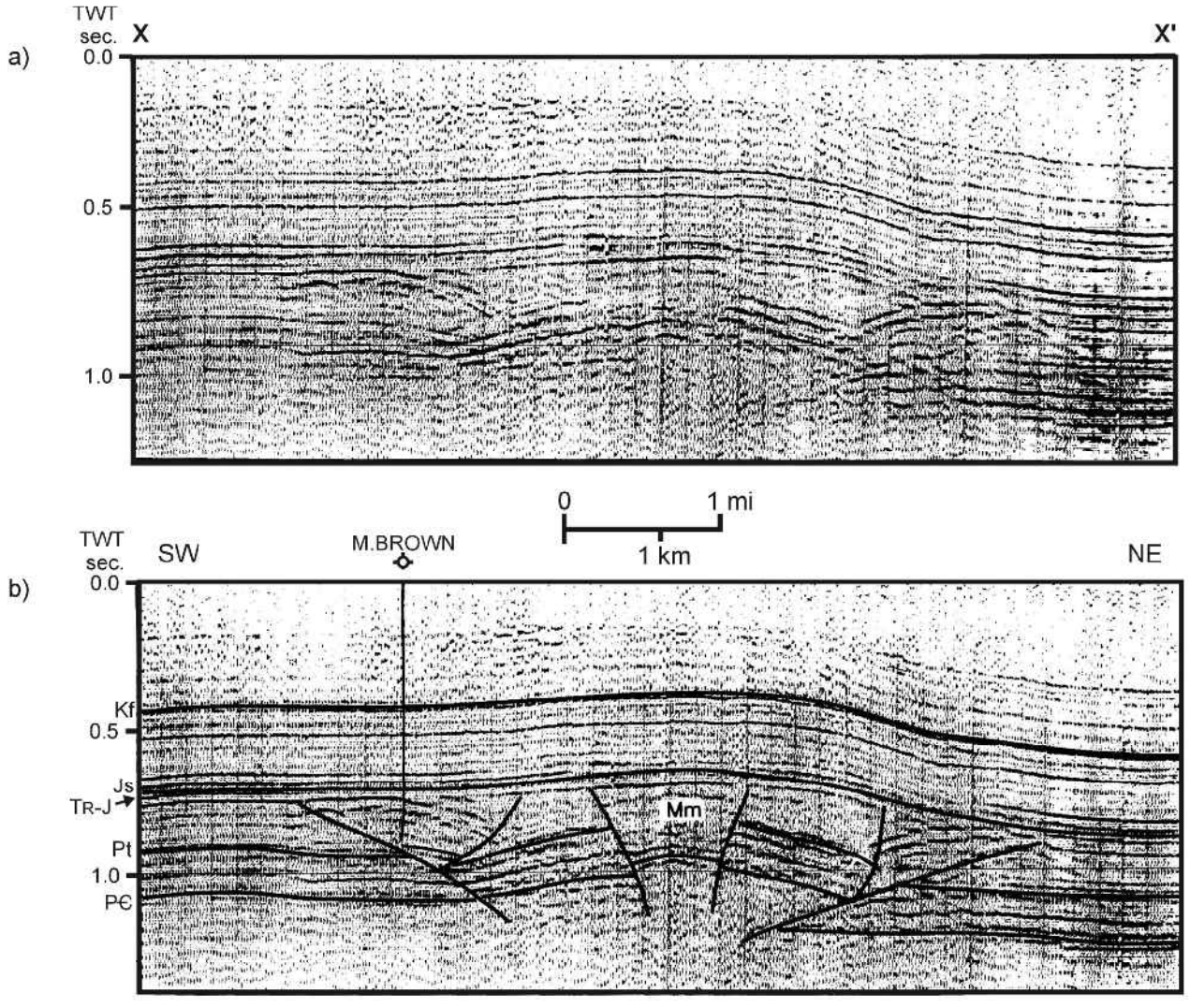

Fig. 7. Unmigrated seismic profile X-X′ (location in Fig. 2): a) uninterpreted, and b) interpreted. Scale is ~1:1. The Tensleep contour horizon of Fig. 2 is marked by the Pt symbol. Other formation symbols are identified on Fig. 3. The dry-hole symbol represents the M. Brown borehole (Nr 10 in Table 1) drilled on the southern rim anticline. TWT is two-way time in seconds. (Modified from Stone 1999.)

and by the onlapping relationship of Sundance members over the buried-hill topography of the central peak. Thus, it is conceivable that prior to erosion at the TR-J unconformity, SU measurement at a higher stratigraphic level (e.g., in the Tensleep Formation) might have approached the ~10% of the restored crater diameter suggested by others (Grieve and Pilkington 1996; French 1998).

The listed 1.4 km diameter of the central peak is near the typical value of 22% (Melosh 1989) of the 7 km diameter of the crater. Note however, if the equations given in Therriault, Grieve, and Reimold (1997) are used, a diameter of ~7 km would yield an SU of 638 m and a central peak diameter of 2.2 km (taken at the base of the central peak, which is usually the widest value). It is certainly possible that the true diameter of the central peak at its base may be greater than the ~1.4 km reported here. The discrepancy is related to the interpreted, inward-dipping faulting shown encircling Cloud Creek's central peak. According to this latter interpretation, central peak diameter decreases with depth.

SAMPLES

Samples from five of the boreholes drilled into the Cloud Creek structure (Table 1) are archived at the U.S. Geological Survey Core Library in Lakewood, Colorado. However, except for a few small core chips in borehole nr 3, only drill cuttings are available for inspection. (This clearly eliminates any possibilities of identifying shatter cones.) The search for quartz grains in these cuttings was particularly difficult as the samples are dirty mixtures of small fragments that include a high percentage of recirculated material. In three half-day visits to the Core Library facility, and using a binocular

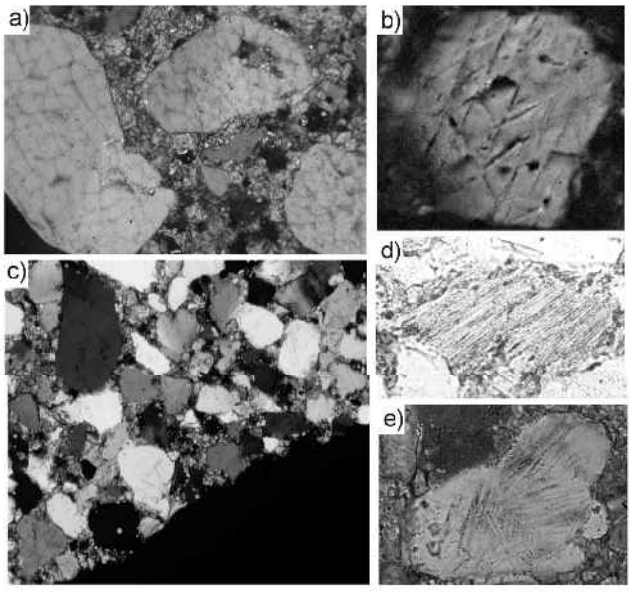

Fig. 8. Photomicrographs of thin section of drill cuttings from: a) fractured pattern in quartz grains at depth interval 5230–5235′ (1594–1596 m) in borehole H. Brown Govt 1 (nr 2 in Table 1 and Figs. 2 and 5; cross-polarized light; field of view = 0.25 mm); b) planar fractures in a quartz grain at depth interval 4000–4010′ (1219–1223 m) in borehole Breitburn Eng. Lost Dome (nr 9 in Table 1 and Figs. 2 and 5; cross-polarized light; field of view = 0.25 mm); c) a breccia fragment at depth interval 3940–3955′ (1200–1205 m) in borehole Delaney State #1 (nr 3 in Table 1 and Figs. 2, 3, and 5), drilled near the central peak of the Cloud Creek structure (cross-polarized light; field of view = 2 mm); d) shocked quartz grain with one set of PDFs running NE-SW at 4915′ (1499 m) depth in borehole Delaney State #1 (nr 3 in Table 1 and Figs. 2, 3, and 5; plane-polarized light; field of view = 0.15 mm); and e) shocked quartz grain with multiple sets of PDFs at depth interval 3940–3955′ (1200–1205 m) in borehole Delaney State #1 (nr 3 in Table 1 and Figs. 2, 3, and 5; cross-polarized light with quartz plate inserted; field of view = 0.25 mm).

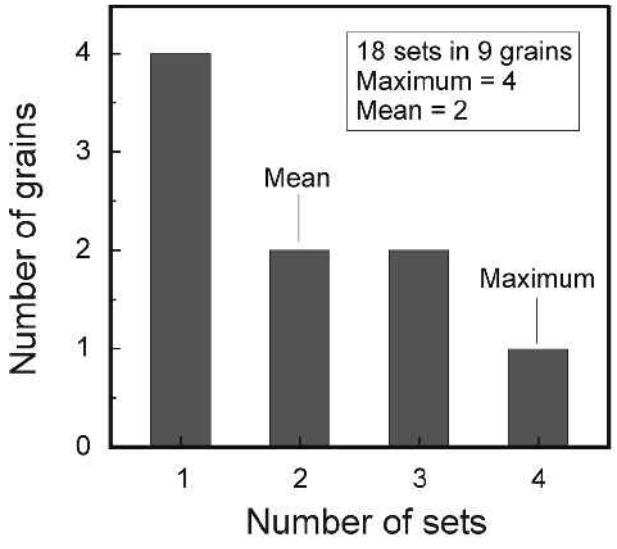

Fig. 9. Histogram of the number of sets of PDFs per individual quartz grain from breccia fragments of the Cloud Creek structure, Wyoming.

microscope (with up to 20× power), cutting fragments were selected from the sample suites from each of the four boreholes marked by asterisks in Table 1. Standard thin sections were ground from selected drill cutting fragments so that a search could be made for shock-metamorphic evidence. Lithologies of these samples vary according to their formational source; but the breccia samples contain a variety of lithologies and individual grains. If collected from the area of the central peak (borehole nr 2; Table 1; Figs. 2, 3, and 5), then the selected samples are primarily Paleozoic marine carbonates (limestone, dolomite, and anhydrite), shales, and minor fine-grained sandstones mixed in with a high proportion of recirculated Cretaceous and Jurassic dark marine shale fragments. If collected from boreholes drilled in the area of the annular trough or rim anticline (boreholes 3, 5, 6, and 9; Table 1; Figs. 2 and 5), the samples range from non-marine, Triassic red shales, mudstones, and siltstones in the upper (younger) crater section to Paleozoic carbonates and fine (Tensleep) sandstones in the lower crater section just above total depth in most of these boreholes. Four thin sections were made from samples collected from borehole nrs. 2 and 9 (Table 1), and 9 thin sections from borehole nr 3 samples. No thin sections were made from boreholes nr 5 and 6, as the samples from these boreholes did not contain recognizable quartz grains in the target intervals.

Planar deformation features (PDFs) in quartz have been identified and measured in samples collected from reported intervals 30 m and 330 m below the TR-J unconformity in the Atlantic Refining Delaney State #1 borehole (nr 3, Table 1; Figs. 2 and 3; and marked with a dry-hole symbol outlined by a black rectangle in Fig. 5b). This borehole was drilled off the southern edge of the central peak, ~1 km southeast of the center of the structure, where the stratigraphic section below the TR-J unconformity is primarily composed of Triassic red shales and siltstones and is structurally "disturbed" or chaotic. Specifically, the Triassic Chugwater stratigraphic interval (beginning below the TR-J unconformity at 1173 m on the spontaneous-potential/resistivity log and extending to 1356 m at the top of the Permian Goose Egg Formation) penetrated in this borehole is anomalously thin and lacks the log correlation markers normally identifiable within this formation.

The sample bags containing the sample fragments from which thin sections were made that yielded shock-metamorphic evidence were labeled 3940–3955 ft (1200–1205 m) and 4905–4915 ft (1495–1498 m). The first interval is stratigraphically just above two ~10 m thick, "out-of-place" sandstones that were cored and are identified on wireline logs within the upper part of the fractured and/or brecciated Triassic Chugwater section in the Atlantic Refining Delaney State #1 borehole (nr 3). Based on examination of the few preserved core chips recovered from these sandstones, the sandstones are interpreted here as exotic slabs of Pennsylvanian Tensleep Formation probably derived (toppled over?) from the central peak. Shock features were found in

the labeled drill cuttings but not in the core chips cut from the sandstones just below the reported drill cuttings interval.

The deeper cutting samples (and the thin section ground from them) labeled 4905–4914 ft (1495–1498 m) would indicate that these samples were collected from near the top of the Pennsylvanian Tensleep Sandstone, which was penetrated near the bottom of the Atlantic Refining borehole (nr 3, Fig. 5b). This label implies that these samples were collected while coring was in progress from a depth of 4895 to 4954 ft (1492 to 1510 m), a coring interval that includes the labeled sample interval. Therefore, it is likely that these drill cutting samples do not represent the depth interval indicated, but may be recirculated fragments from a shallower depth. Moreover, examination of the few archived core chips from this deeper cored interval did not reveal any shock features.

Shock metamorphic microstructures (discussed below) and microstructures more common to regional metamorphic deformation have been identified in samples not only from borehole nr 3, but also from borehole nrs. 2 and 9. These include irregular prismatic fracture patterns or cleavage in quartz grains (Fig. 8a), observed in the upper sections of some boreholes, and may be attributable to the shock event (e.g., Stöffler and Langenhorst 1994). Also observed are metamorphic deformation lamellae (or Boehm lamellae), which consist of irregular planar trails of micro-inclusions more or less parallel and generally slightly to highly curved. These deformation lamellae are virtually parallel and closely spaced and two or more sets may be present at different angles, which are not parallel to any definite crystallographic plane of quartz but all appear to be at low angles to the c-axis or (0001).

SHOCK METAMORPHISM

Planar fractures were observed in very few quartz grains (Fig. 8b), but were not measured. As shown in Figure 8b, these microstructures are parallel sets of open fissures with a typical spacing of more than 20 µm. Most shock metamorphic effects observed in quartz occur as planar deformation features (PDFs), no shock effects typical of a high-pressure regime (e.g., diaplectic glass and high-pressure polymorphs) have been identified. Of all thin sections on hand, PDFs in shocked quartz grains were measured in two thin sections of drill cutting samples from the labeled depth intervals of 3940–3955 ft (1200–1205 m) and 4905–4915 ft (1495–1498 m) in borehole nr 3, the Atlantic Refining Delaney State #1 (Table 1; Figs. 2, 3, and 5). These thin sections contain mainly sandstone and breccia fragments (Fig. 8c). A total of 18 PDF sets in 9 grains, with a mean of 2 sets per grain and a maximum of 4 sets in one grain (Table 1 and Fig. 9), were measured using a universal stage mounted on a Leitz binocular, transmitted light microscope. We should point out that the samples containing PDFs recovered from the Atlantic Refining borehole (nr 3) represent a small percent of the total number of samples collected, sorted, viewed in oil under a petrographic microscope, selected for thin sectioning, and studied by a number of knowledgeable petrologists (see Stone 1999). Considering the poor quality of the sample material, this result is not unexpected. The low quartz grains number is due to the limited amount of material available and reflects that less than 5% of the grains in the thin sections studied contain PDFs. These shocked quartz grains range in size from 0.3 to 0.5 mm and have a straight to undulatory extinction, resulting in an error of <5° for the c-axis orientation. Individual PDF lamellae are decorated, more or less sharp, straight to slightly curved, cover 100% of the grain, and have a spacing of 1 to 5 µm between individual planes (e.g., Figs. 8d and 8e).

All PDF sets were indexed to crystallographic planes of quartz using a template (with 5° circles around each pole of the crystallographic planes; Stöffler and Langenhorst 1994) over the stereonet plot (Wulff net projection) of each quartz grain to obtain their best fit. This method allows for a certain correction of the c-axis and PDF measurement errors (not always taken into account when using only a standard histogram plot) and retains the angular and directional relationship between PDF sets. Sets of PDF were assigned to specific crystallographic planes according to the best fit obtained (Table 3 and Fig. 10). In cases where only one PDF set was measured in a quartz grain, these PDFs correspond to only one specific group of crystallographic planes (i.e., ω at 23° or π at 32°). Results indicate one marked peak (Fig. 10), corresponding to the ω $\{10\bar{1}3\}$ crystallographic plane of quartz with 50% (9) of the measured PDF sets falling within ±5° of 23°. The presence of relatively abundant ω and π orientations indicate that moderate to high shock pressures, ranging between 20 and 25 GPa (Robertson and Grieve 1977; Langenhorst and Deutsch 1994; Stöffler and Langenhorst 1994), affected the target rocks of the central peak during formation of these PDFs. The crystallographic orientations distribution shown in Fig. 10 for the Cloud Creek structure,

Table 3. Crystallographic orientations of indexed PDFs measured in shocked quartz grains from the Cloud Creek structure, as obtained from stereonet plots. Data used in Figure 12.

Orientation	Miller-Bravais index	Polar angle with c-axis	Number of PDF sets	Percentage
ω	$\{10\bar{1}3\}$	23°	9	50.0%
π	$\{10\bar{1}2\}$	32°	4	22.2%
ξ	$\{10\bar{2}2\}$	48°	3	16.7%
r, z	$\{10\bar{1}1\}$, $\{01\bar{1}1\}$	52°	2	11.1%
			Total = 18 sets	

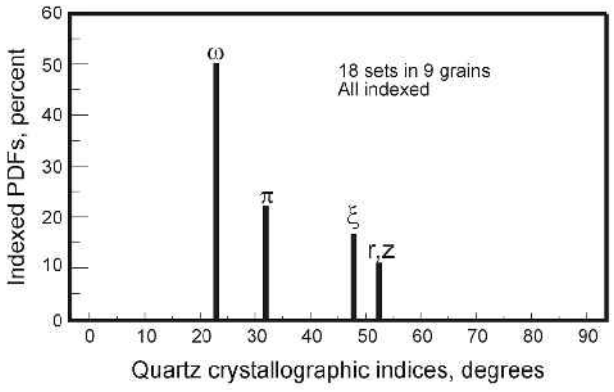

Fig. 10. Histogram of the frequency of indexed PDFs in quartz grains in relation to quartz crystallographic indices for the Cloud Creek structure, Wyoming. See text for details.

even though the actual number of PDF orientations measured is relatively low, corresponds to that found at confirmed impact structures formed in consolidated rocks with low porosity (e.g., Grieve, Langenhorst, and Stöffler 1996). This is in agreement with the local geology.

SUMMARY AND CONCLUSIONS

The morphologic and morphometric data recorded at Cloud Creek are comparable with those reported in studies of other well-preserved, complex terrestrial impact structures in (predominantly) sedimentary target rocks, e.g., the Red Wing Creek structure in North Dakota (Brenan, Peterson, and Smith 1975; Koeberl, Reimold, and Brandt 1996). Furthermore, in the absence of any evidence of volcanic activity, igneous intrusion, caldera or maar formation, salt tectonics or solution collapse, or intersecting wrench-fault ("pop-up") tectonics, an endogenic origin for the Cloud Creek structure can be ruled out (Stone 1999). With the addition of the shock-metamorphic and other petrographic evidence reported here, the Cloud Creek structure is now considered confirmed as a complex impact structure, about 7 km in diameter, formed sometime between the Late Triassic and Middle Jurassic (i.e., 190 ± 20 Ma).

Acknowledgments–We would like to thank R. A. F. Grieve for a review of this work in its earliest form and his constructive comments. Contributions of many individuals, operating oil companies, and geophysical service companies are acknowledged by the senior author in Stone 1999, but Mark Longman and Matt Morgan deserve special thanks for their generous contributions to the petrographic studies. Final revision based on critical reviews by David Kring and Bevan French greatly improved the manuscript. This paper is Geological Survey of Canada Contribution 2002105.

Editorial Handling—Dr. Richard Grieve

REFERENCES

Blackstone D. L., Jr. 1990. Rocky Mountain foreland structure exemplified by the Owl Creek Mountains, Bridger Range, and Casper Arch, central Wyoming. In *Wyoming sedimentation and tectonics,* edited by Specht R. W. Casper: Wyoming Geological Association. pp. 151–166.

Brenan R. L., Peterson B. J., and Smith H. J. 1975. The origin of Red Wing Creek structure: McKenzie County, North Dakota. *Wyoming Geological Association Earth Science Bulletin* 8:1–41.

Brown W. G. 1993. Structural style of basement-cored uplifts and associated folds. In *Geology of Wyoming*, edited by Snoke A. W., Steidtman J. R., and Roberts S. M. Laramie: Wyoming State Geological Survey. pp. 313–371.

French B. M. 1998. *Traces of catastrophe: A handbook of shock-metamorphic effects in terrestrial meteorite impact structures.* LPI Contribution No. 954. Houston: Lunar and Planetary Institute. 120 p.

Grieve R. A. F. 1991. Terrestrial impact: The record in the rocks. *Meteoritics* 26:175–194.

Grieve R. A. F. and Pilkington M. 1996. The signature of terrestrial impact craters. *AGSO Journal of Australian Geology and Geophysics* 16:399–420.

Grieve R. A. F., Langenhorst F., and Stöffler D. 1996. Shock metamorphism of quartz in nature and experiment: II. Significance in geoscience. *Meteoritics* 31:6–35.

Koeberl C., Reimold W. U., and Brandt D. 1996. Red Wing Creek structure, North Dakota: Petrographical and geochemical studies and confirmation of impact origin. *Meteoritics & Planetary Science* 31:335–342.

Langenhorst F. and Deutsch A. 1994. Shock experiments on α- and β-quartz: I. Optical and density data. *Earth and Planetary Science Letters* 125:407–420.

Melosh H. J. 1989. *Impact cratering. A geologic process.* New York: Oxford University Press. 245 p.

Pilkington M. and Grieve R. A. F. 1992. The geophysical signature of terrestrial impact craters. *Review of Geophysics* 30:161–181.

Pipiringos G. N. and O'Sullivan R. B. 1978. Principal unconformities in Triassic and Jurassic rocks, western interior Unites States—A preliminary survey. *U.S. Geological Survey Professional Paper 1035-A*. 29 p.

Robertson P. B. and Grieve R. A. F. 1977. Shock attenuation at terrestrial impact structures. In *Impact and explosion cratering*, edited by Roddy D. J., Pepin R. O., and Merril R. B. New York: Pergamon Press. pp. 687–702.

Skeen R. C. and Ray R. R. 1983. Seismic models and interpretation of the Casper Arch thrust: Applications to Rocky Mountain foreland structure. In *Rocky Mountain basins and uplifts*, edited by Lowell J. D. Denver: Rocky Mountain Association of Geologists. pp. 99–124.

Stöffler D. and Langenhorst F. 1994. Shock metamorphism of quartz in nature and experiment: I. Basic observation and theory. *Meteoritics* 29:155–181.

Stone D. S. 1969. Wrench faulting and Rocky Mountain tectonics. *The Mountain Geologist* 6:67–79.

Stone D. S. 1993. Basement-involved thrust-generated folds as seismically imaged in the subsurface of the central Rocky Mountain foreland. In *Laramide basement deformation in the Rocky Mountain Foreland of the western United States*, edited by Schmidt C. J., Chase R. B., and Erslev E. A. GSA Special Publication 280. Boulder: Geological Society of America. pp. 271–318.

Stone D. S. 1999. Cloud Creek: A possible impact structure on the Casper Arch, Wyoming. *The Mountain Geologist* 36:211–234.

Stone D. S. 2002. Morphology of the Casper Mountain uplift and

related, subsidiary structures, central Wyoming: Implications for Laramide kinematics, dynamics, and crustal inheritance. *American Association of Petroleum Geologists Bulletin* 86: 1417–1440.

Therriault A. M., Grieve R. A. F., and Reimold W. U. 1997. Original size of the Vredefort structure: Implications for the geological evolution of the Witwatersrand Basin. *Meteoritics & Planetary Science* 32:71–77.

Thompson G. A. and Hill J. L. 1986. The deep crust in convergent and divergent terranes: Laramide uplifts and basin-range rifts. *Reflection seismology: The continental crust*, edited by Barazangi M. and Brown L. Washington DC: American Geophysical Union. pp. 243–256.